Detecting earlier stages of amyloid deposition using PET in cognitively normal elderly adults

Tengfei Guo, PhD, Susan M. Landau, PhD, and William J. Jagust, MD, for the Alzheimer's Disease Neuroimaging Initiative

Correspondence
Dr. Guo
tengfei.guo@berkeley.edu

Abstract

Objective
To examine the feasibility of using cross-sectional PET to identify cognitive decliners among β-amyloid (Aβ)-negative cognitively normal (CN) elderly adults.

Methods
We determined the highest Aβ-affected region by ranking baseline and accumulation rates of florbetapir-PET regions in 355 CN elderly adults using ^{18}F-florbetapir-PET from the Alzheimer's Disease Neuroimaging Initiative (ADNI). The banks of the superior temporal sulcus (BANKSSTS) were found as the highest Aβ-affected region, and Aβ positivity in this region was defined as above the lowest boundary of BANKSSTS standardized uptake value ratio of Aβ+ (ADNI-defined COMPOSITE region) CN individuals. The entire CN cohort was divided as follows: stage 0, BANKSSTS−COMPOSITE−; stage 1, BANKSSTS+COMPOSITE−; and stage 2, BANKSSTS+COMPOSITE+. Linear mixed-effect (LME) models investigated subsequent longitudinal cognitive change, and ^{18}F-flortaucipir (FTP)-PET was measured 4.8 ± 1.6 years later to track tau deposition.

Results
LME analysis revealed that individuals in stage 1 (n = 64) and stage 2 (n = 99) showed 2.5 ($p < 0.05$) and 4.8 ($p < 0.001$) times faster memory decline, respectively, than those in stage 0 (n = 191) over >4 years of mean follow-up. Compared to stage 0, both stage 1 ($p < 0.05$) and stage 2 ($p < 0.001$) predicted higher FTP in entorhinal cortex.

Conclusions
Nominally Aβ− CN individuals with high Aβ in BANKSSTS are at increased risk of cognitive decline, probably showing an earlier stage of Aβ deposition. Our findings may help elucidate the association between brain Aβ accumulation and cognition in Aβ− CN cohorts.

Classification of evidence
This study provides Class II evidence that in elderly CN individuals those with high PET-identified superior temporal sulcus Aβ burden have an increased risk of cognitive decline.

Glossary

Aβ = β-amyloid; **AD** = Alzheimer disease; **ADNI** = Alzheimer's Disease Neuroimaging Initiative; **BANKSSTS** = banks of the superior temporal sulcus; **CN** = cognitively normal; **FDG** = ^{18}F-fluorodeoxyglucose; **FTP** = ^{18}F-flortaucipir; **GLM** = generalized linear models; **GMM** = gaussian mixed-model; **LME** = linear mixed-effect; **p-tau** = phosphorylated tau; **PCC** = posterior cingulate cortex; **ROI** = region of interest; **SUVR** = standardized uptake value ratio; **t-tau** = total tau.

The presence of widespread cortical β-amyloid (Aβ) is regarded as the initial event that leads to Alzheimer disease (AD)[1] and occurs in ≈30% of cognitively normal (CN) elderly adults >70 years of age.[2] Recent failures of clinical trials in patients with AD[3–6] have moved therapeutic interventions to Aβ+ CN elderly adults. Two recent studies reported that memory decline occurred even in Aβ− CN individuals who appear to be accumulating Aβ.[7,8] However, it is still unclear how to identify those Aβ− individuals with cognitive decline using cross-sectional PET.

Regional Aβ deposition[9–12] and Aβ accumulation rate[10,13–15] vary across region. Thus, a standardized uptake value ratio (SUVR) in a composite cortical area[16] (referred to as the COMPOSITE region) is often used to evaluate cerebral Aβ deposition. The highest Aβ-affected region may accumulate more Aβ than other regions over the same period,[17] reflecting either increased biological vulnerability or simply greater measurement sensitivity for the detection of Aβ deposition, which may be a good indicator of earlier Aβ accumulation compared to the global COMPOSITE region.

In this study, we determined the highest Aβ-affected region in CN elderly adults using baseline and longitudinal ^{18}F-florbetapir-PET, and we used this region to differentiate individuals who may have biologically significant Aβ accumulation from other Aβ− CN individuals. We investigated whether Aβ− CN individuals with high Aβ burden in the highest Aβ-affected region have faster rates of cognitive decline than those with low Aβ burden.

Methods

Participants

The data were obtained from the Alzheimer's Disease Neuroimaging Initiative (ADNI) database (ida.loni.usc.edu). The participants in this study were 355 ADNI participants who were CN and had a florbetapir-PET scan structural MRI at baseline and had ≥2 subsequent longitudinal cognitive testing sessions.

Standard protocol approvals, registrations, and patient consents

The ADNI study was approved by institutional review boards of all participating centers, and written informed consent was obtained from all participants or their authorized representatives.

Florbetapir-PET image acquisition and analysis

Details on florbetapir image acquisition are given elsewhere (adni-info.org). Baseline and follow-up florbetapir scans were coregistered to baseline structural MRI scans. Cortical retention in 34 FreeSurfer-defined regions of interest (ROIs) and a composite reference region (made up of brainstem, whole cerebellum, and eroded white matter) was calculated with FreeSurfer (version 5.3.0) as described previously.[18] This reference region was chosen because it has shown stability in longitudinal analyses, as we planned.[18] SUVR was calculated as a ratio of regional florbetapir to that in the reference region. The SUVR from a COMPOSITE region was averaged to create a cortical summary SUVR.[16] The Aβ positivity of the COMPOSITE region was defined as SUVR ≥0.82, which corresponds to the previously validated whole cerebellum–based florbetapir positivity threshold of 1.11[16] and was derived with the regression equation ($y = 0.64 \times x + 0.14$) that resulted from correlating whole cerebellum–normalized cortical summary SUVR (x-axis) against the composite-reference-normalized cortical summary SUVR (y-axis) for 1,216 ADNI individuals with a baseline florbetapir-PET scan. Annual rates of SUVR (SUVR unit per year) were calculated for each individual with linear regression.

Top Aβ-affected cortical regions

The spatial and temporal patterns of Aβ were studied in globally Aβ− and Aβ+ CN elderly adults. Mean baseline SUVRs and rates of SUVR change in 34 ROIs[19] were calculated across participants and compared with the COMPOSITE region. We determined regions with significantly higher SUVRs and faster rates of SUVR increase than the COMPOSITE region. The highest SUVR also was compared with other ROIs. A false discovery rate of 0.05 with the Benjamini-Hochberg approach[20] was used for multiple-comparisons correction. To confirm the presence of Aβ pathology, regions with the highest baseline SUVRs in the Aβ+ participants were defined as the top Aβ-affected regions, indicating the most measurement sensitivity for the detection of Aβ deposition. Random sampling test without replacement was used to assess the generalizability of these regions. We randomly selected 50% of Aβ+ participants with baseline florbetapir-PET scans as sample A, while the remaining 50% of participants were used as sample B. The consistency of top Aβ-affected regions between sample A and sample B was compared. We did these analyses for 5,000 iterations.

To confirm the consistency of top Aβ-affected regions in Aβ− participants, we also examined top baseline SUVRs in Aβ− participants in the same manner as in Aβ+ participants. For each iteration in the random sampling test of Aβ− participants, we randomly selected 50% of Aβ− participants with baseline florbetapir-PET scans as sample C, while the remaining 50% of

Aβ− participants were used as sample D among 5,000 iterations. In addition, we assessed the top rates of SUVR increase in both Aβ− and Aβ+ participants to examine how fast they are accumulating Aβ.

Staging amyloidosis

As defined, top Aβ-affected regions should not be negative in the Aβ+ CN population; thus, regional Aβ positivity thresholds were defined as being above the lowest boundary (first percentile) of the corresponding SUVRs in the Aβ+ CN group. For comparison, we also used gaussian mixed-model (GMM) analysis to estimate 2 gaussian distributions of low Aβ and high Aβ for the highest Aβ-affected region ($Region_{highest}$) to define an unsupervised threshold, which corresponds to a 90% probability of belonging to the high-Aβ distribution.

The highest Aβ-affected region ($Region_{highest}$) was used to classify the entire group of CN participants into 3 different amyloidosis stages according to the thresholds of $Region_{highest}$ and COMPOSITE regions: stage 0, $Region_{highest}$−/COMPOSITE−; stage 1, $Region_{highest}$+/COMPOSITE−; and stage 2, $Region_{highest}$+/COMPOSITE+.

To examine whether the COMPOSITE region alone could yield information similar to the $Region_{highest}$, we also used GMM analysis to estimate 2 gaussian distributions of low Aβ and high Aβ for COMPOSITE SUVRs, and a low threshold was defined as an SUVR corresponding to a 90% probability of belonging to the low-Aβ distribution.[21] Individuals with SUVRs of COMPOSITE below the low threshold, above or equal to the low threshold but <0.82, and ≥0.82 were defined as stages 0, 1, and 2, respectively.

Cognitive tests

Previously validated longitudinal memory and executive function composite scores that were derived from the ADNI neuropsychological battery were used in this study.[22,23] The memory composite score was calculated by combining different cognitive scores, including the Auditory Verbal Learning Test, the word list learning and recognition components of Alzheimer's Disease Assessment Scale–Cognitive Subscale, word recall items from the Mini-Mental State Examination, and Logical Memory I from the Wechsler Memory Test–Revised. The executive function composite score was calculated by combining digit symbol substitution and digit span backward tests, Trail Making Test Parts A and B, animal and vegetable Category Fluency, Digit Cancellation, and the Clock Drawing test. More details can be found on the ADNI website (ADNI_Methods_UWNPSYCHSUM_20160112.pdf). Annual rates of memory and executive function decline were calculated for each participant on the basis of longitudinal memory and executive scores using linear regression.

Comparisons of other biomarkers at different amyloidosis stages

CSF biomarkers (Aβ$_{1–42}$, total tau [t-tau], and phosphorylated tau [p-tau]) (n = 279), structural MRI (n = 333), and

^{18}F-fluorodeoxyglucose (FDG)-PET (n = 351) acquired within 1 year of the baseline florbetapir scan were compared at different stages. Because the baseline florbetapir scan had no concurrent ^{18}F-flortaucipir (FTP) data, we compared the closest subsequent FTP-PET data (n = 149) at different stages. The mean interval between baseline florbetapir scan and the closest FTP scan was 4.83 ± 1.55 years.

CSF Aβ$_{1–42}$, t-tau, and p-tau measurements were analyzed by the ADNI Biomarker core laboratory via the Roche Elecsys platform, as described on the ADNI website (ADNI_UPENN_CSF_Biomarkers_Elecsys_METHODS_20170411.pdf). FTP SUVRs in entorhinal ROIs were calculated on the basis of mean uptake over 80 to 100 minutes after injection normalized by a mean inferior cerebellar gray matter uptake[24] in native space after partial volume correction. Hippocampal volume was obtained from the structural MRI concurrent with the baseline florbetapir scan with FreeSurfer and adjusted by intracranial volume with the regression approach.[25] Mean ^{18}F-FDG uptake within a set of predefined and previously validated ROIs (metaROI) was calculated as described elsewhere in detail.[16] Generalized linear models (GLMs) compared CSF biomarkers, FTP SUVR in entorhinal and hippocampal volume, and FDG SUVR in different amyloidosis stages, controlling for *APOE* ε4 status, age, sex, and education.

Association between rate of cognition and regional SUVRs of top Aβ-affected regions in Aβ− cohort

GLMs were used to investigate the predictive effect of SUVRs of the top Aβ-affected regions at predicting annual rates of memory and executive function decline across participant in the Aβ− CN cohort, controlling for *APOE* ε4 status, age, sex, and education. GLM models with different top Aβ-affected regions were compared by use of the Akaike information criterion.

Statistical analysis

Normality of distributions was tested with the Shapiro-Wilk test and visual inspection of data histograms. Data are presented as mean ± SD. Given a normal distribution of variables, a 2-tailed *t* test at the significance level of $p < 0.05$ was applied if not otherwise noted. Linear mixed-effects (LME) models were used to investigate subsequent longitudinal change of memory and executive function over time (lme4 package) on the basis of the following independent variables: time, stage, stage × time, *APOE* ε4 status, age, sex, and education, and including a random slope and intercept for each participant. Participants with faster rates of memory or executive function decline than the median rate of the whole CN cohort were defined as memory or executive function decliners. The percentages of memory and executive function decliners were compared among different amyloidosis stages with the Fisher exact test. All the statistical analyses were conducted in the statistical program R (version 3.6.1, R Foundation for Statistical Computing, Vienna, Austria).

Data availability

All data are available in the ADNI database (ida.loni.usc.edu). Derived data are available from the corresponding author on request by any qualified investigator.

Results

Demographics

At baseline, 355 CN (255 Aβ− and 100 Aβ+ by the COMPOSITE region) participants had at least 1 florbetapir-PET scan and ≥2 longitudinal cognitive evaluations. In addition, 220 Aβ− and 83 Aβ+ CN participants had ≥2 florbetapir-PET scans, and 150 Aβ− and 50 Aβ+ had ≥3 florbetapir-PET scans. At baseline, the Aβ+ group was older ($p \leq 0.017$) and had significantly higher SUVRs and more *APOE* ε4 carriers ($p < 0.001$) than the Aβ− group in both cross-sectional and longitudinal cohorts.

Top Aβ-affected cortical regions

As shown in figure 1A, 12 regions showed higher SUVR (paired-sample *t* test, $p < 0.03$) than the COMPOSITE region in Aβ+ participants. The highest SUVR region was the banks of the superior temporal sulcus (BANKSSTS, figure 1C), followed by posterior cingulate cortex (PCC) and precuneus. BANKSSTS had a higher ($p < 0.001$) SUVR than the other 11 regions. In the random sampling test, BANKSSTS showed the highest SUVR in both samples A and B (each made up of 50% of Aβ+ participants) among all 5,000 iterations; PCC showed the second highest SUVR in sample A in 99.4% (4,970 of 5,000) of the iterations and in sample B in 99.5% (4,977 of 5,000) of the iterations; and precuneus showed the third highest SUVR in sample A in 98.2% (4,909 of 5,000) of the iterations and in sample B in 98.0% (4,901 of 5,000) of the iterations. BANKSSTS also showed the highest SUVR in Aβ− participants in sample C in 99.7% (4,984 of 5,000) of the iterations and in sample D in 99.7% (4,983 of 5,000) of the iterations in the random sampling test.

Precuneus, inferior temporal, BANKSSTS, PCC, and middle temporal regions had faster ($p < 0.05$) rates of SUVR increase than the COMPOSITE region based on the 83 Aβ+ participants with ≥2 florbetapir scans (figure 1B). In 50 Aβ+ participants with ≥3 florbetapir scans, BANKSSTS, precuneus, and middle and inferior temporal regions had faster ($p < 0.05$) rates of SUVR than the COMPOSITE region. In addition, PCC, precuneus, isthmus cingulate, and BANKSSTS had faster ($p < 0.05$) rates of SUVR increase than the COMPOSITE region among the 220 Aβ− participants with ≥2 florbetapir scans and the 150 Aβ− participants with ≥3 florbetapir scans.

As described above, BANKSSTS, precuneus, and PCC regions were the top Aβ-affected regions; thus, we limited the following analyses to these regions. The highest Aβ-affected region, BANKSSTS, was selected to stage amyloidosis in the CN cohort. For comparison with BANKSSTS, the analyses using the second and third highest PCC and precuneus and the COMPOSITE region with a lower Aβ+ threshold to stage amyloidosis are also summarized.

Staging amyloidosis using the BANKSSTS

The Aβ positivity threshold for BANKSSTS was calculated as an SUVR of 0.904, and participants were classified into stages 0 to 2 as described. Only 1 of the 355 total participants was BANKSSTS−/COMPOSITE+; this individual was removed from the analysis. Relationships between the classifications by the 2 ROIs are shown in figure 1D.

Demographic characteristics at baseline are summarized in the table for each group. Stage 2 participants had significantly higher SUVRs, lower memory and executive function composite scores, older ages, and higher percentage of *APOE* ε4 carriers than the participants at the other 2 stages. Stages 2 and 1 had higher ($p < 0.02$) percentages of females than stage 0. In addition, stage 1 had higher SUVRs ($p < 0.001$) than stage 0, but no other difference was found between stage 0 and stage 1.

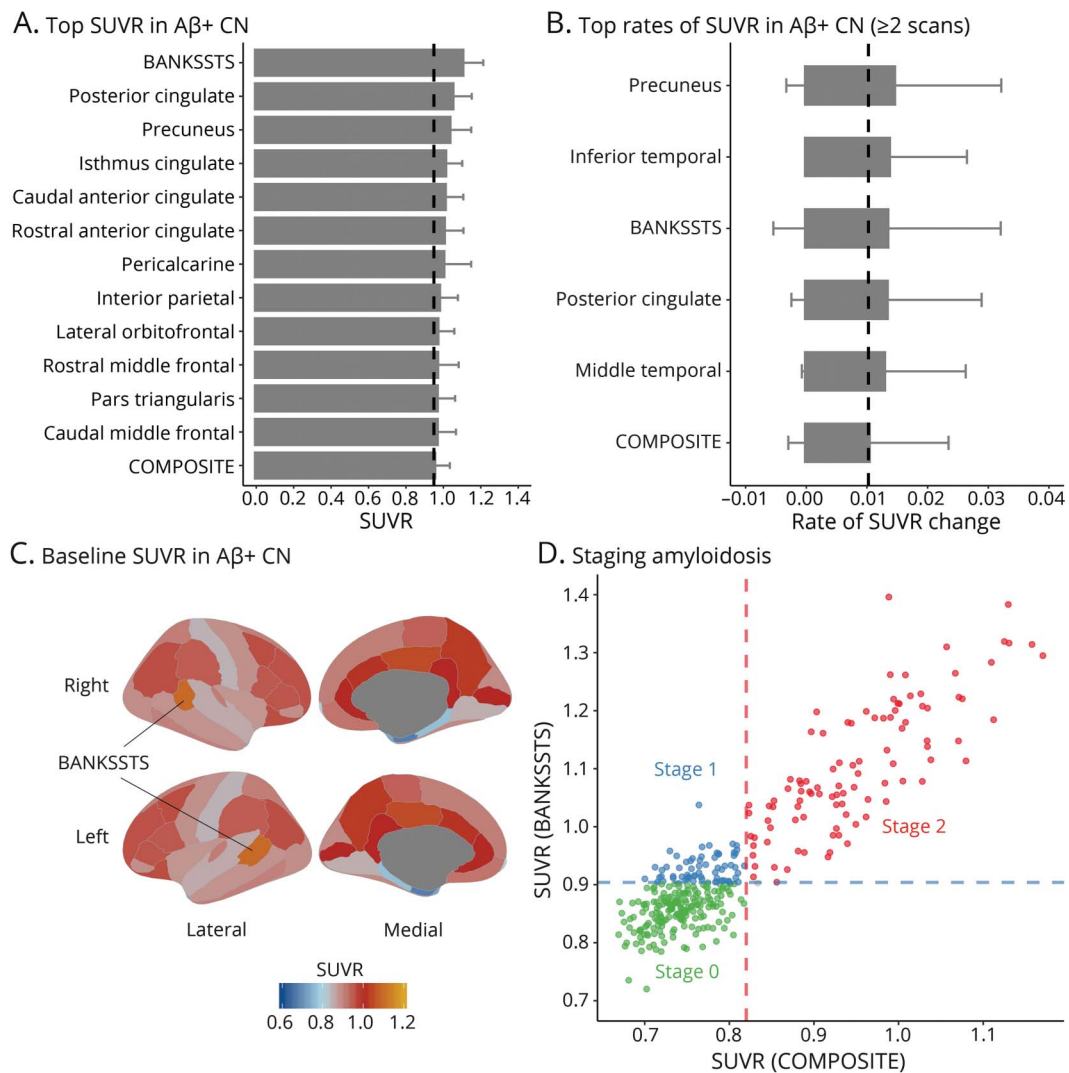### Comparison of cognitive decline at different amyloidosis stages

LME models revealed that all 3 stages showed rates of memory decline significantly different from zero over ≈4 years of mean follow-up (figure 2A). Rates of memory decline at stages 1 and 2 were 2.5 ($p = 0.028$) and 4.8 ($p < 0.001$) times faster, respectively, than at stage 0; the rate of memory decline at stage 2 was also faster ($p = 0.004$) than at stage 1. Stage 1 ($p = 0.040$) and stage 2 ($p < 0.001$) showed rates of executive function decline significantly different from zero, although stage 0 ($p = 0.220$) had no significant executive function decline (figure 2B). The rate of executive function decline at stage 2 was faster ($p = 0.001$) than at stage 0, while no significant difference ($p = 0.094$) was found between stages 1 and 2.

The percentages of memory decliners at stage 1 (58% [37 of 64], $p = 0.009$) and stage 2 (66% [66 of 99], $p < 0.001$) were significantly higher than at stage 0 (39% [74 of 191]), whereas the percentages of executive function decliners at stage 1 (50% [32 of 64]) and stage 2 (57% [56 of 99]) were not significantly higher than at stage 0 (46% [88 of 191]).

Comparisons of other biomarkers at different amyloidosis stages

Participants in stage 2 (n = 82) had lower CSF Aβ$_{1-42}$ and higher CSF t-tau and CSF p-tau than those in stage 1 (n = 48, $p < 0.001$) and stage 0 (n = 149, $p < 0.001$); participants in stage 1 had lower ($p < 0.05$) CSF Aβ$_{1-42}$ than those in stage 0, but no differences were found in CSF t-tau or p-tau (figure 3, A–C). In entorhinal cortex, stage 2 participants (n = 40) showed marginally higher ($p < 0.1$) FTP SUVR than stage 1 participants (n = 33) and higher ($p < 0.001$) FTP SUVR than those in stage 0 (n = 76), and those in stage 1 also had higher ($p < 0.05$) FTP SUVR than participants in stage 0 (figure 3D). Those in stage 2 (n = 93) had marginally lower hippocampal volume than participants in stage 1 (n = 59, $p < 0.1$) and lower hippocampal

Figure 1 Top Aβ-affected regions and amyloidosis stages defined by the highest region and COMPOSITE region

(A) Top regions with significantly higher standardized uptake value ratios (SUVRs) than the COMPOSITE region based on 100 β-amyloid (Aβ)–positive cognitively normal (CN) participants. (B) Top regions with significantly faster rates of SUVR change than the COMPOSITE region based on 83 Aβ+ CN participants with at least 2 florbetapir-PET scans. Black dashed line denotes the corresponding value of the COMPOSITE region. (C) Mean baseline SUVRs of 68 FreeSurfer-defined regions of interest in Aβ+ CN participants. (D) Amyloidosis stages defined by thresholds of the banks of the superior temporal sulcus (BANKSSTS) and COMPOSITE. Blue and red dash lines denote the thresholds of SUVR in BANKSSTS and COMPOSITE, respectively. Green, blue, and red dots denote stage 0 (BANKSSTS−/COMPOSITE−), stage 1 (BANKSSTS+/COMPOSITE−), and stage 2 (BANKSSTS+/COMPOSITE+), respectively.

volume than those in stage 0 (n = 181, $p < 0.05$), while no differences were found between participants in stages 1 and 0 (figure 3E). Likewise, those in stage 2 (n = 99) had significantly lower glucose metabolism than those in stage 0 ($p < 0.05$, n = 189), while no differences were found in other comparisons (figure 3F).

Transitioning of amyloidosis stages at follow-up

The longitudinal results were consistent with the definition of the amyloidosis stages based on cross-sectional data, such that BANKSSTS was consistently elevated relative to the COMPOSITE region. Stage 0 participants were most likely to first transition to stage 1 and then progress to stage 2 (figure 4A). Individuals who did not follow this pattern and initially transitioned from stage 0 to stage 2 had baseline SUVRs very close to the COMPOSITE threshold. Stage 1 participants were more likely (32% [18 of 56] vs 9% [15 of 164], Fisher exact test, $p < 0.001$) to transition to stage 2 over >4 years of mean follow-up than stage 0 participants.

Of 164 stage 0 participants, 114 remained stage 0, 30 progressed to stage 1, 9 progressed to stage 1 and then to stage 2, 6 progressed directly to stage 2, and 5 progressed to BANK-SSTS−/COMPOSITE+ at follow-up (figure 4B). The probability of stage 0 participants first crossing the BANKSSTS threshold (39 of 50) was higher (exact binominal test, $p < 0.001$) than the probability of stage 0 participants directly crossing the COMPOSITE threshold (11 of 50). Of 56 participants classified as stage 1 at baseline, 25 remained stage 1, 18 transitioned to stage 2, and 13 changed to stage 0 at follow-up

Table Demographic characteristics at baseline of participants at different amyloidosis stages

	Stage 0 (n = 191)	Stage 1 (n = 64)	Stage 2 (n = 99)
SUVR (COMPOSITE)	0.74 ± 0.03	0.77 ± 0.03[a]	0.95 ± 0.08
SUVR (BANKSST)	0.85 ± 0.03	0.93 ± 0.02	1.10 ± 0.11[b]
Memory composite score	1.12 ± 0.59	1.19 ± 0.63	0.93 ± 0.59[c]
Executive function score	0.93 ± 0.84	0.97 ± 0.72	0.64 ± 0.67[c]
Follow-up of cognition, y	4.12 ± 1.70	4.54 ± 1.85	3.89 ± 1.66
Age, y	74.16 ± 6.79	73.53 ± 6.08	76.56 ± 6.10[d]
Education, y	16.82 ± 2.68	16.25 ± 2.26	16.11 ± 2.74
M/F, n	104/87	23/41[e]	39/60[e]
APOE ε4, %	17.28	26.56[f]	46.46[g]

Abbreviations: BANKSSTS = banks of the superior temporal sulcus; SUVR = standardized uptake value ratio.
[a] Significantly higher than stage 0, Mann-Whitney test, $p < 0.001$.
[b] Significantly higher than stage 1, Mann-Whitney test, $p < 0.001$.
[c] Significantly lower memory and executive function than stages 0 and 1, 2-sample t test, $p < 0.01$.
[d] Significantly older than stages 0 and 1, 2-sample t test, $p < 0.003$.
[e] Significantly higher percentage of female than stage 0, Fisher exact test, $p < 0.02$.
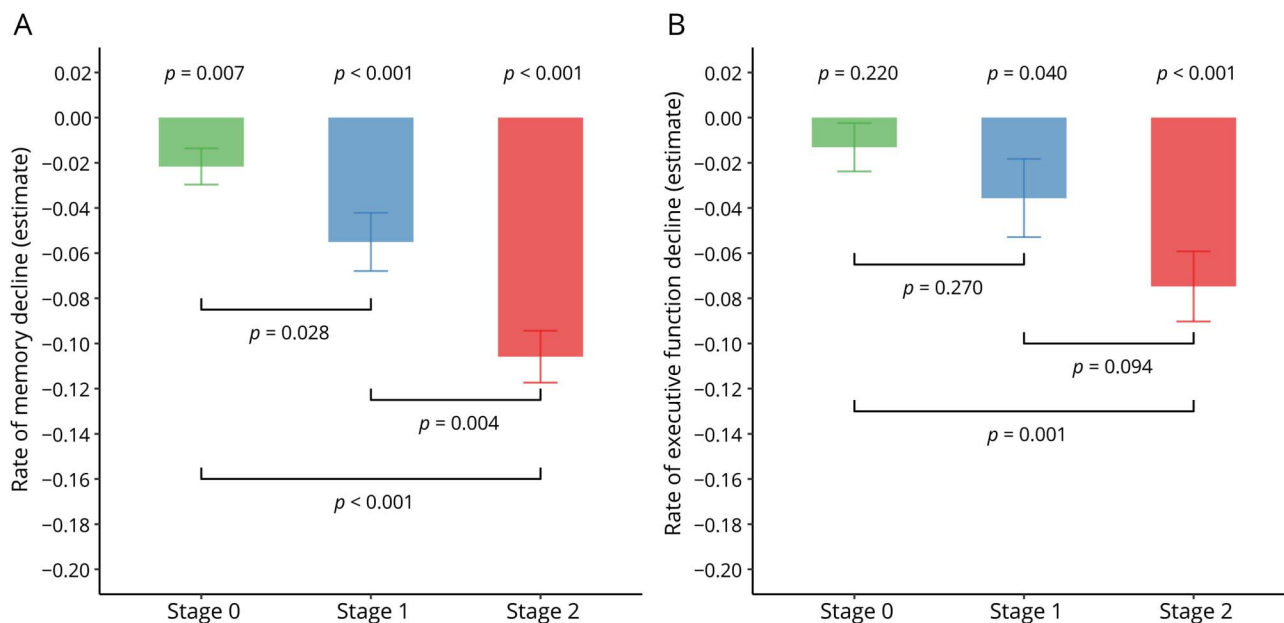[f] Higher percentage of _APOE_ ε4 carriers than stage 0, Fisher exact test, $p = 0.14$.
[g] Significantly higher percentage of _APOE_ ε4 carriers than stages 0 and 1, Fisher exact test, $p < 0.014$.

(figure 4C). Note that 10 of 13 stage 1 participants who changed to stage 0 at follow-up also decreased in the COMPOSITE SUVR. Of 82 stage 2 participants, 78 remained stage 2, 1 individual changed from stage 2 to stage 1 to 0, 2 individuals changed from stage 2 to stage 1, and 1 individual changed from stage 2 to BANKSSTS−/COMPOSITE+ at follow-up (figure 4D).
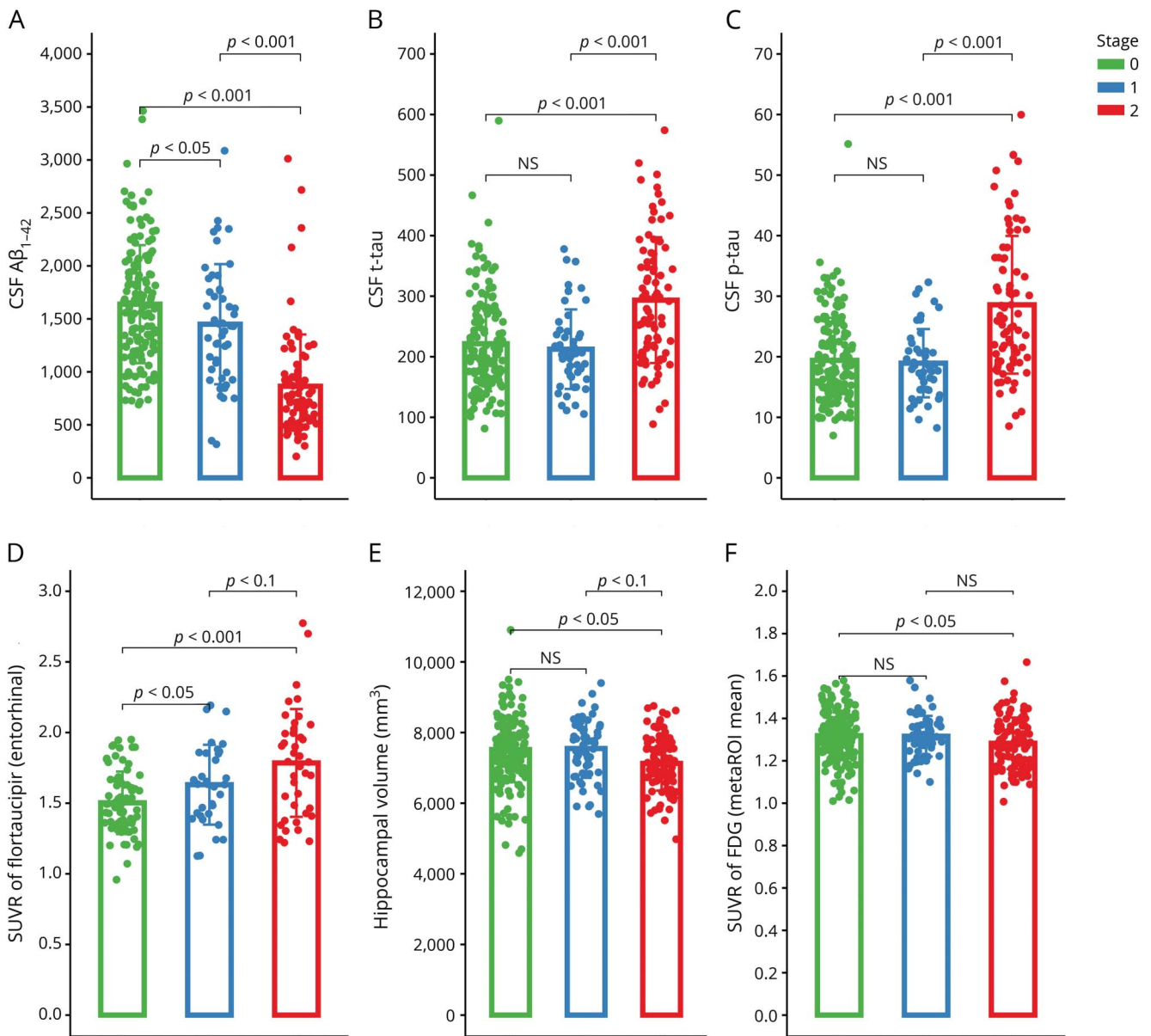
Staging amyloidosis by using the BANKSSTS with an alternative thresholding approach

An alternative Aβ positivity threshold of BANKSSTS (0.895) was calculated from GMM analysis based on 355 CN individuals as described (figure 5A). Of 355 CN individuals, 174, 81, and 100 were classified as stages 0, 1, and 2, respectively (figure 5B). LME models revealed that all 3 stages showed rates

Figure 2 Longitudinal changes of memory and executive function over time in different amyloidosis stages

(A) Comparisons of rates of memory decline at different amyloidosis stages. (B) Comparisons of rates of executive function decline at different amyloidosis stages. The p values above the bar reflect the comparison between rates of cognitive decline and zero. Bar and error bar denote the estimate of mean and standard error from the linear mixed-effect models.

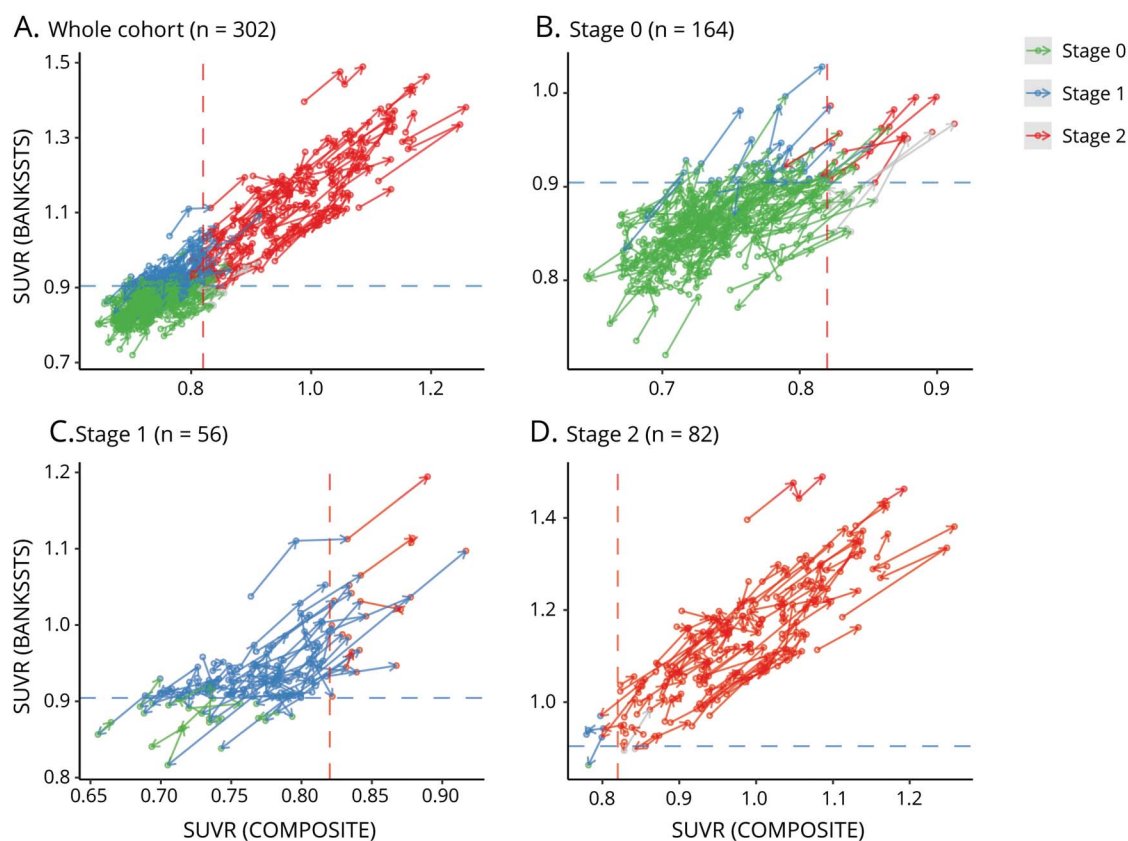**Figure 3** Comparisons of CSF biomarkers, tau PET, hippocampal volume, and FDG-PET in different amyloidosis stages

Comparison of baseline (A) CSF β-amyloid (Aβ)$_{1-42}$, (B) CSF total tau (t-tau), (C) CSF phosphorylated tau (p-tau) (interval from baseline florbetapir: mean 0.04 ± 0.10, range 0–0.96, unit year; stage 0, n = 149; stage 1, n = 48; stage 2, n = 82), and (D) standardized uptake value ratio (SUVR) of flortaucipir in entorhinal ≈4.83 years after baseline florbetapir-PET scan (interval from baseline florbetapir: mean 4.83 ± 1.55, range 0–7.40, unit year; stage 0, n = 76; stage 1, n = 33; stage 2, n = 40), (E) adjusted hippocampal volume (interval from baseline florbetapir: mean 0.03 ± 0.16, range 0–1.00, unit year; stage 0, n = 181; stage 1, n = 59; stage 2, n = 93), and (F) SUVR of ^{18}F-fluorodeoxyglucose (FDG) in predefined and previously validated ROI (metaROI) (interval from baseline florbetapir: mean 0.03 ± 0.09, range 0–1.00, unit year; stage 0, n = 189; stage 1, n = 63; stage 2, n = 99) at different amyloidosis stages. Bar and error bar denote mean and SD. NS = no significance.

of memory decline significantly different from zero over ≈4 years of mean follow-up (figure 5C). Rates of memory decline at stages 1 and 2 were 2.4 ($p = 0.036$) and 4.9 ($p < 0.001$) times faster, respectively, than at stage 0; the rate of memory decline at stage 2 was also faster ($p = 0.002$) than at stage 1 (figure 5C). Stage 1 ($p = 0.031$) and stage 2 ($p < 0.001$) showed rates of executive function decline that were significantly different from zero, although stage 0 ($p = 0.287$) had no significant executive function decline (figure 5D). The rate of executive function decline at stage 2 was faster ($p = 0.001$) than at stage 0, while no

significant difference ($p = 0.070$) was found between stages 1 and 2 (figure 5D). The comparisons of CSF Aβ$_{1-42}$, t-tau and p-tau, FTP SUVR in entorhinal and hippocampal volume, and hypometabolism at different stages defined by the lenient threshold of 0.895 were similar to that using the threshold of 0.904. However, stage 1 did not show lower CSF Aβ$_{1-42}$ and only marginally ($p = 0.061$) higher FTP SUVR in entorhinal 4.8 years after baseline florbetapir scan than stage 0, which may be because 17 more Aβ− CN individuals were pooled to stage 1 according to the lenient threshold of BANKSSTS.

Figure 4 Transition of amyloidosis stages from different initial stage

Transitioning of amyloidosis stage of (A) whole longitudinal cohort, (B) stage 0 participants at baseline, (C) stage 1 participants at baseline, and (D) stage 2 participants at baseline. Arrows reflect temporal sequence of PET scans. BANKSSTS = banks of the superior temporal sulcus; SUVR = standardized uptake value ratio.

Staging amyloidosis using other regions

Corresponding thresholds of Aβ positivity in PCC and precuneus were calculated as SUVRs of 0.867 and 0.833, respectively, with the same approach (SUVRs corresponding to the first percentile in the Aβ+ CN group) as we did for BANKSSTS. With the use of the PCC and COMPOSITE regions, 219, 36, and 99 were classified as stages 0, 1, and 2, respectively. Likewise, 220, 35, and 99 were classified as stages 0, 1, and 2 when precuneus and COMPOSITE region were used. Using PCC and precuneus to stage amyloidosis, we also observed marginal or significant rates of memory and executive function decline at stage 1, but the rates of memory and executive function decline at stage 1 were not significantly faster than at stage 0.

GMM analysis defined a low threshold for COMPOSITE region as an SUVR 0.79, which corresponds to a 90% probability of belonging to the low-Aβ distribution (figure 6A). Staging amyloidosis was also examined with the use of a low threshold of SUVR 0.79 in the COMPOSITE region. Of 355 CN individuals, 220, 35, and 100 were classified as stages 0, 1, and 2 with the thresholds 0.79 and 0.82 of COMPOSITE region. All the stages showed rates of memory decline significantly greater than zero (figure 6B). Stages 0 and 2 showed rates of executive function decline significantly greater than zero, but stage 1 had
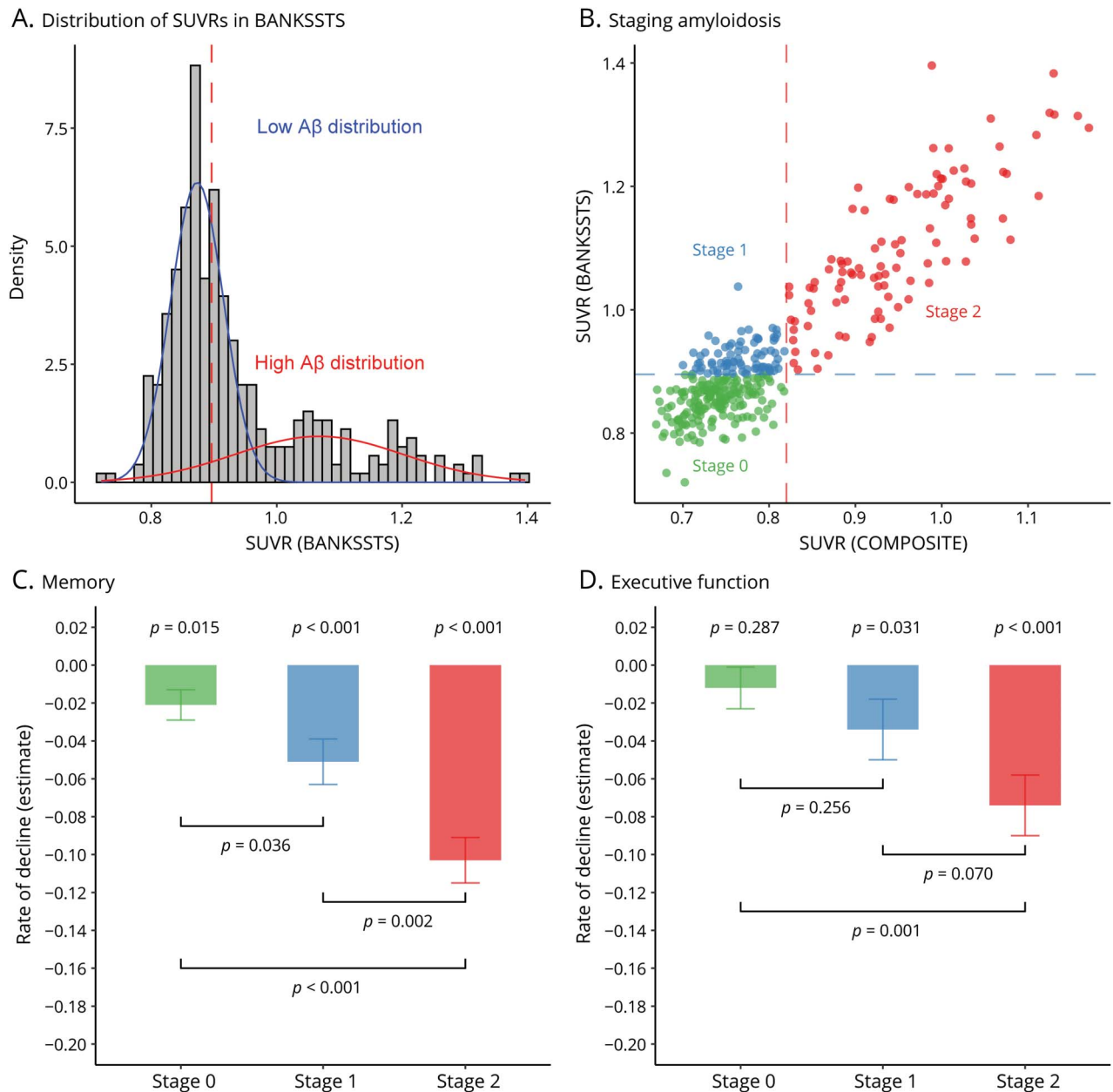
no significant negative rate of executive function decline (figure 6C). Stage 2 had a faster rate of decline in memory (figure 6B) and executive function (figure 6C) than stages 0 and 1 over >4 years of mean follow-up. However, no significant difference was found in the rate of either memory or executive function decline between stages 0 and 1 (figure 6, B and C).

The comparisons of CSF $A\beta_{1-42}$, t-tau and p-tau, FTP SUVR in entorhinal and hippocampal volume, and hypometabolism at different stages defined by PCC, precuneus, and COMPOSITE with a low threshold were similar to that at different stages defined by BANKSSTS except that no significant difference was found in FTP SUVR between stages 0 and 1.

Association between rate of cognition and regional SUVRs of top Aβ-affected regions in Aβ− cohort

Continuously, GLM models revealed that only BANKSSTS SUVR showed a significant ($p = 0.024$) association with the rate of memory decline in 255 Aβ− participants, and BANKSSTS also had lower Akaike information criterion than PCC and precuneus. None of them showed a significant association between baseline SUVR and rate of executive function decline.

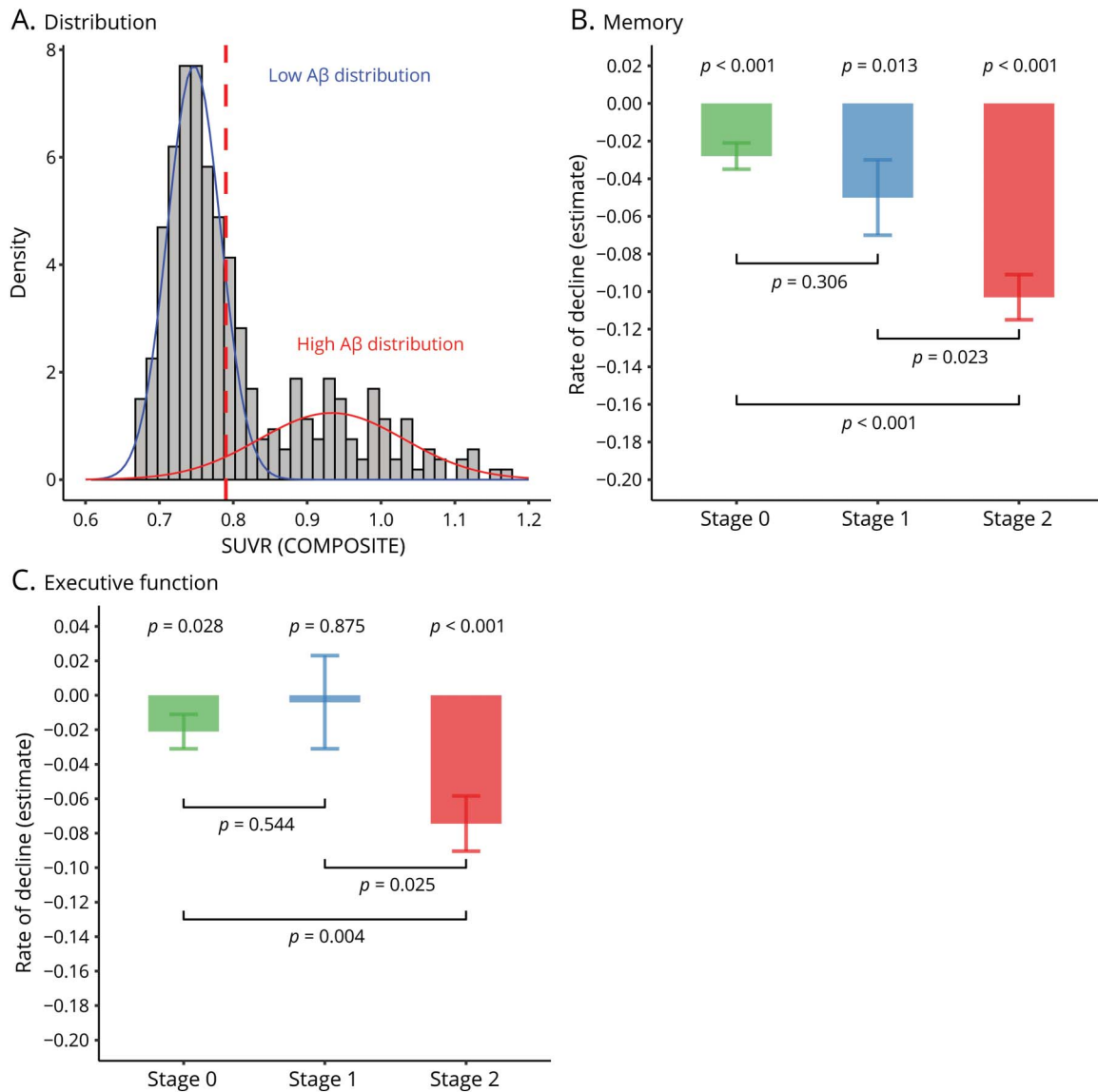**Figure 5** Analyses by using the threshold of BANKSSTS SUVR derived from an unsupervised method

(A) Estimates of 2 gaussian distributions of low β-amyloid (Aβ) (blue curve) and high Aβ (red curve) for the banks of the superior temporal sulcus (BANKSSTS) standardized uptake value ratios (SUVRs) of 355 cognitively normal participants. Red dashed vertical line reflects the Aβ+ threshold of BANKSSTS 0.895, which corresponds to a 90% probability of belonging to the high-Aβ distribution. (B) Amyloidosis stages defined by SUVR in BANKSSTS and COMPOSITE. Comparisons of longitudinal change in (C) memory and (D) executive function at different amyloidosis stages.

Discussion

Our results showed that BANKSSTS is the highest Aβ-affected cortical region in both Aβ− and Aβ+ CN participants and appears more sensitive to detect early Aβ deposition than the COMPOSITE region. Nominally Aβ− CN participants with high Aβ burden in BANKSSTS are probably at an intermediate amyloidosis stage, with a greater risk of cognitive decline than participants who did not show Aβ burden in this region.

Consistent with our findings, we identified other regions with elevated Aβ (BANKSSTS, PCC, and precuneus) that have also been reported as early Aβ-accumulating regions in a previous study,[26] although BANKSSTS was not explicitly reported in their table 2. One recent longitudinal study also found that BANKSSTS, PCC, and precuneus showed the fastest rates of Aβ accumulation at a very early stage in mutation carriers of autosomal dominant AD,[27] and BANKSSTS was also among the earliest regions to show glucose hypometabolism and

(A) Estimates of 2 gaussian distributions of low β-amyloid (Aβ) (blue curve) and high Aβ (red curve) for COMPOSITE standardized uptake value ratios (SUVRs) of 355 cognitively normal participants. Red dashed vertical line reflects the Aβ+ threshold of COMPOSITE 0.79, which corresponds to a 90% probability of belonging to the low-Aβ distribution. Comparisons of longitudinal change in (B) memory and (C) executive function at different amyloidosis stages.

cortical atrophy. In addition, the superior temporal sulcus shows very early neuropathologic involvement[28] and discriminates individuals with mild memory impairment who progress to AD from those who do not.[29] In contrast, a recent cross-sectional study estimated the frequency of regional Aβ positivity using the COMPOSITE for multiple brain regions and found that early Aβ accumulation most frequently occurred in inferior temporal, fusiform, anterior cingulate, and parietal operculum.[30] However, use of the same global threshold in each brain region might not be the best way to capture the regional Aβ positivity because in our data regional thresholds are not identical.

We observed that stage 2 had faster rates of memory decline than stages 0 and 1 over ≈4 years of mean follow-up, which

was consistent with previous studies.[31–41] Stage 1 had 2.5 times the rate of memory decline compared to stage 0. In addition, we found significant executive function decline at stages 1 and 2. Faster executive function decline is consistent with previous studies.[31–34,39,40]

In contrast, stage 1 (PCC+/COMPOSITE− and precuneus+/COMPOSITE−) defined by the second (PCC) and third (precuneus) highest Aβ-affected regions did not show significantly faster rates of cognitive decline than stage 0 (PCC−/COMPOSITE− and precuneus−/COMPOSITE−). Consequently, PCC, precuneus, or a composite region (BANKSSTS, PCC and precuneus) may be less sensitive than BANKSSTS in detecting early Aβ positivity. Using the COMPOSITE region with a lower Aβ+ threshold to stage amyloidosis also did not

predict cognitive decline as well as BANKSSTS (figure 6, B and C), implying that regional Aβ may be more sensitive to detect Aβ-related cognitive change than global Aβ in Aβ− CN cohorts. In line with our findings, Farrell et al.[8] recently reported that regional rather than global longitudinal SUVR increase predicted memory decline in Aβ− CN elderly adults, although BANKSSTS was not evaluated.

Stage 2 had significantly higher CSF p-tau and CSF t-tau and lower hippocampal volume and metabolism (figure 3) than stages 1 and 0; however, no significant differences were found between stages 0 and 1, suggesting that BANKSSTS+ participants are less progressed than COMPOSITE+ participants and not notably different than those at stage 0 in terms of neurodegenerative and CSF tau biomarkers. High Aβ burden at stages 2 and 1 predicted significantly higher FTP SUVR in entorhinal cortex than stage 0 ≈4.8 years later, which was consistent with a previous study.[42] Our results support the hypothetical temporal order of the AD pathologic cascade.[1] More important, those findings also imply that amyloid-lowering interventions may have more potential treatment effect on stage 1 CN participants than stage 2 CN participants or patients with cognitive impairment,[43] because stage 1 participants showed significant Aβ-related cognitive decline but had no evidence of neurodegeneration yet.

The large sample size of longitudinal PET data in our study enables us to validate the proposed sequence of amyloidosis stages that were defined using regional and composite cross-sectional data. Aβ− CN individuals are most likely to progress following stage 0 → stage 1 → stage 2 (figure 4). We found that some stage 0 individuals whose SUVRs were very close to the threshold of the COMPOSITE progressed to BANKSSTS−COMPOSITE+ and then transitioned to stage 2 (figure 4B), but the percentage of those individuals was low (6.7%). Most of the 114 stable stage 0 participants will likely transition to stage 1 first. Thirteen stage 1 individuals changed to stage 0 at follow-up (figures 4C), and 10 of them also decreased in the SUVR of the COMPOSITE region, suggesting that they were in an unstable amyloid state. Because 3 participants changed their amyloid status on the basis of the BANKSSTS region and not the COMPOSITE region, it is possible that BANKSSTS may have less stable measurement properties, which seems likely because of its smaller size.

One recent study used the striatum and COMPOSITE region to identify individuals at a late amyloidosis stage[44] and found that COMPOSITE+/striatum+ (10% of CN cohort) participants showed a faster rate of cognitive decline than COMPOSITE+/striatum− participants. Unlike that study, we suggest using cross-sectional PET data to identify individuals who have accumulated biologically significant Aβ burden but have not yet reached the threshold of COMPOSITE+, which is relevant for the selection of target participants in early stages for antiamyloid drug trials. Together, these results suggest that the highest Aβ-affected region may be more helpful for identifying individuals with risk of Aβ-related cognitive decline than the COMPOSITE region in the early amyloidosis stage, while the COMPOSITE region or striatum may perform better at selecting individuals who are at a late amyloidosis stage on the AD continuum. The selection of approaches for evaluating brain Aβ deposition really depends on the aims of research or clinical intervention in CN elderly adults.

Previous studies reported that CSF $A\beta_{1-42}$[45] or a CSF ratio with $A\beta_{1-42}$[46] can predict early PET Aβ accumulation in PET− CN cohort, but in these studies, neither CSF $A\beta_{1-42}$ nor a CSF ratio with $A\beta_{1-42}$ was associated with cognitive decline, perhaps because the progression of AD is preferentially associated with amyloid PET.[47–49] According to our approach, 25% of the Aβ− CN cohort was detected as stage 1 by amyloid PET, showing significantly faster rate of memory decline than stage 0 participants, although the magnitude of rate of cognitive decline at stage 1 was only ≈50% of stage 2, presumably because it was so early.

One limitation of this study is that the highest Aβ-affected regions and their corresponding thresholds of Aβ positivity were defined on the basis of the ADNI database, which requires validation with other databases. Second, although stage 1 participants appear to be developing Aβ pathology according to >4 years of mean follow-up, even longer follow-up periods would be useful to assess the continuity of amyloid accumulation in these individuals. Third, it would be very helpful to validate the superior predictive effect of BANKSSTS for subsequent memory decline compared to other top regions in other samples. Finally, it is possible that a multivariate approach to define early brain regions might be more sensitive than our method in detecting a constellation of regions or voxels that best predict cognitive or biomarker outcomes.

Nominally Aβ− CN individuals with high florbetapir uptake in BANKSSTS are at increased risk of cognitive decline, probably showing an earlier stage of Aβ deposition. Our findings may help elucidate the association between brain Aβ accumulation and cognition in Aβ− CN cohort and provide an approach to identify suitable early-stage patients for amyloid-lowering interventions.

Study funding

Disclosure

T. Guo reports no disclosures relevant to the manuscript. S.M. Landau has served as a consultant to Cortexyme and NeuroVision. W.J. Jagust has served as a consultant to Genentech, Novartis, Bioclinica, and Biogen. Go to Neurology.org/N for full disclosures.

Publication history

Appendix 1 Authors

Name	Location	Contribution
Tengfei Guo, PhD	University of California, Berkeley	Study design, drafting and editing the manuscript, data and statistical analysis, and interpretation of results
Susan M. Landau, PhD	University of California, Berkeley	Interpretation of results, obtaining funding, editing the manuscript, and study supervision
William J. Jagust, MD	University of California, Berkeley	Interpretation of results, obtaining funding, editing the manuscript, and study supervision

Appendix 2 Coinvestigators

Name	Location	Role	Contribution
Michael W. Weiner, MD	University of California, San Francisco	Director of coordinating center	Led and coordinated communication among sites of ADNI
John Q. Trojanowski, MD, PhD	University of Pennsylvania, Philadelphia	Site investigator	Coordinated biomarker core
Leslie Shaw, PhD	University of Pennsylvania, Philadelphia	Site investigator	Coordinated biomarker core
Laurel Beckett, PhD	University of California, Davis	Site investigator	Coordinated biostatistics core
Paul Aisen, MD	University of Southern California, Los Angeles	Site investigator	Coordinated clinical core

Appendix 2 *(continued)*

Name	Location	Role	Contribution
Ronald Petersen, MD, PhD	Mayo Clinic, Rochester, MN	Site investigator	Coordinated clinical core
Andrew J. Saykin, PsyD	Indiana University, Indianapolis	Site investigator	Coordinated genetics core
Arthur W. Toga, PhD	University of Southern California, Los Angeles	Site investigator	Coordinated informatics core
Clifford Jack, MD	Mayo Clinic, Rochester, MN	Site investigator	Coordinated MRI core
John C. Morris, MD	Washington University, St. Louis, MO	Site investigator	Coordinated neuropathology core
William Jagust, MD	University of California, Berkeley	Site investigator	Coordinated PET core

References

1. Jack CR, Knopman DS, Jagust WJ, et al. Tracking pathophysiological processes in Alzheimer's disease: an updated hypothetical model of dynamic biomarkers. Lancet Neurol 2013;12:207–216.
2. Roberts RO, Aakre JA, Kremers WK, et al. Prevalence and outcomes of amyloid positivity among persons without dementia in a longitudinal, population-based setting. JAMA Neurol 2018;75:970.
3. Salloway S, Sperling R, Fox NC, et al. Two phase 3 trials of bapineuzumab in mild-to-moderate Alzheimer's disease. N Engl J Med 2014;370:322–333.
4. Doody RS, Thomas RG, Farlow M, et al. Phase 3 trials of solanezumab for mild-to-moderate Alzheimer's disease. N Engl J Med 2014;370:311–321.
5. Egan MF, Kost J, Tariot PN, et al. Randomized trial of verubecestat for mild-to-moderate Alzheimer's disease. N Engl J Med 2018;378:1691–1703.
6. Liu E, Schmidt ME, Margolin R, et al. Amyloid-β 11 C-PiB-PET imaging results from 2 randomized bapineuzumab phase 3 AD trials. Neurology 2015;85:692–700.
7. Landau SM, Horng A, Jagust WJ. Memory decline accompanies subthreshold amyloid accumulation. Neurology 2018;90:e1452–e1460.
8. Farrell ME, Chen X, Rundle MM, Chan MY, Wig GS, Park DC. Regional amyloid accumulation and cognitive decline in initially amyloid-negative adults. Neurology 2018;91:e1809–e1821.
9. Rinne JO, Brooks DJ, Rossor MN, et al. 11C-PiB PET assessment of change in fibrillar amyloid-β load in patients with Alzheimer's disease treated with bapineuzumab: a phase 2, double-blind, placebo-controlled, ascending-dose study. Lancet Neurol 2010;9:363–372.
10. Villemagne VL, Pike KE, Chételat G, et al. Longitudinal assessment of Aβ and cognition in aging and Alzheimer disease. Ann Neurol 2011;69:181–192.
11. Wong DF, Rosenberg PB, Zhou Y, et al. In vivo imaging of amyloid deposition in Alzheimer disease using the radioligand 18F-AV-45 (flobetapir F 18). J Nucl Med 2010;51:913–920.
12. Barthel H, Gertz HJ, Dresel S, et al. Cerebral amyloid-β PET with florbetaben (18F) in patients with Alzheimer's disease and healthy controls: a multicentre phase 2 diagnostic study. Lancet Neurol 2011;10:424–435.
13. Villain N, Chételat G, Grassiot B, et al. Regional dynamics of amyloid-β deposition in healthy elderly, mild cognitive impairment and Alzheimer's disease: a voxelwise PiB-PET longitudinal study. Brain 2012;135:2126–2139.
14. Guo T, Brendel M, Grimmer T, Rominger A, Yakushev I. Predicting regional pattern of longitudinal β-amyloid accumulation by baseline PET. J Nucl Med 2017;58:639–645.
15. Guo T, Dukart J, Brendel M, Rominger A, Grimmer T, Yakushev I. Rate of β-amyloid accumulation varies with baseline amyloid burden: implications for anti-amyloid drug trials. Alzheimers Dement 2018;14:1387–1396.
16. Landau SM, Mintun MA, Joshi AD, et al. Amyloid deposition, hypometabolism, and longitudinal cognitive decline. Ann Neurol 2012;72:578–586.
17. Whittington A, Sharp DJ, Gunn RN. Spatiotemporal distribution of β-amyloid in Alzheimer disease is the result of heterogeneous regional carrying capacities. J Nucl Med 2018;59:822–827.
18. Landau SM, Fero A, Baker SL, et al. Measurement of longitudinal-amyloid change with 18F-florbetapir PET and standardized uptake value ratios. J Nucl Med 2015;56:567–574.
19. Desikan RS, Ségonne F, Fischl B, et al. An automated labeling system for subdividing the human cerebral cortex on MRI scans into gyral based regions of interest. Neuroimage 2006;31:968–980.

20. Benjamini Y, Hochberg Y. Controlling the false discovery rate: a practical and powerful approach to multiple testing. J R Stat Soc Ser B 1995;57:289–300.
21. Villeneuve S, Rabinovici GD, Cohn-Sheehy BI, et al. Existing Pittsburgh compound-B positron emission tomography thresholds are too high: statistical and pathological evaluation. Brain 2015;138:2020–2033.
22. Crane PK, Carle A, Gibbons LE, et al. Development and assessment of a composite score for memory in the Alzheimer's Disease Neuroimaging Initiative (ADNI). Brain Imaging Behav 2012;6:502–516.
23. Gibbons LE, Carle AC, Mackin RS, et al. A composite score for executive functioning, validated in Alzheimer's Disease Neuroimaging Initiative (ADNI) participants with baseline mild cognitive impairment. Brain Imaging Behav 2012;6:517–527.
24. Maass A, Landau S, Baker SL, et al. Comparison of multiple tau-PET measures as biomarkers in aging and Alzheimer's disease. Neuroimage 2017;157:448–463.
25. Buckner RL, Head D, Parker J, et al. A unified approach for morphometric and functional data analysis in young, old, and demented adults using automated atlas-based head size normalization: reliability and validation against manual measurement of total intracranial volume. Neuroimage 2004;23:724–738.
26. Palmqvist S, Schöll M, Strandberg O, et al. Earliest accumulation of β-amyloid occurs within the default-mode network and concurrently affects brain connectivity. Nat Commun 2017;8:1214.
27. Gordon BA, Blazey TM, Su Y, et al. Spatial patterns of neuroimaging biomarker change in individuals from families with autosomal dominant Alzheimer's disease: a longitudinal study. Lancet Neurol 2018;17:241–250.
28. Gómez-Isla T, Hollister R, West H, et al. Neuronal loss correlates with but exceeds neurofibrillary tangles in Alzheimer's disease. Ann Neurol 1997;41:17–24.
29. Killiany RJ, Gomez-Isla T, Moss M, et al. Use of structural magnetic resonance imaging to predict who will get Alzheimer's disease. Ann Neurol 2000;47:430–439.
30. Grothe MJ, Barthel H, Sepulcre J, Dyrba M, Sabri O, Teipel SJ. In vivo staging of regional amyloid deposition. Neurology 2017;89:2031–2038.
31. Donohue MC, Sperling RA, Salmon DP, et al. The preclinical Alzheimer cognitive composite: measuring amyloid-related decline. JAMA Neurol 2014;71:961–970.
32. Pietrzak RH, Lim YY, Neumeister A, et al. Amyloid-β, anxiety, and cognitive decline in preclinical Alzheimer disease a multicenter, prospective cohort study. JAMA Psychiatry 2015;72:284–291.
33. Clark LR, Racine AM, Koscik RL, et al. Beta-amyloid and cognitive decline in late middle age: findings from the Wisconsin Registry for Alzheimer's Prevention study. Alzheimers Dement 2016;12:805–814.
34. Petersen RC, Wiste HJ, Weigand SD, et al. Association of elevated amyloid levels with cognition and biomarkers in cognitively normal people from the community. JAMA Neurol 2016;73:85–92.
35. Mormino EC, Papp KV, Rentz DM, et al. Early and late change on the preclinical Alzheimer's cognitive composite in clinically normal older individuals with elevated amyloid β. Alzheimers Dement (Amst) 2017;13:1004–1012.
36. Baker JE, Lim YY, Pietrzak RH, et al. Cognitive impairment and decline in cognitively normal older adults with high amyloid-β: a meta-analysis. Alzheimers Dement (Amst) 2018;6:108–121.
37. Donohue MC, Sperling RA, Petersen R, Sun CK, Weiner MW, Aisen PS. Association between elevated brain amyloid and subsequent cognitive decline among cognitively normal persons. JAMA 2017;317:2305.
38. Farrell ME, Kennedy KM, Rodrigue KM, et al. Association of longitudinal cognitive decline with amyloid burden in middle-aged and older adults: evidence for a dose-response relationship. JAMA Neurol 2017;74:830–838.
39. Zhao Y, Tudorascu DL, Lopez OL, et al. Amyloid β deposition and suspected non-Alzheimer pathophysiology and cognitive decline patterns for 12 years in oldest old participants without dementia. JAMA Neurol 2018;75:88–96.
40. Lim YY, Snyder PJ, Pietrzak RH, et al. Sensitivity of composite scores to amyloid burden in preclinical Alzheimer's disease: introducing the Z-scores of attention, verbal fluency, and episodic memory for nondemented older adults composite score. Alzheimers Dement (Amst) 2016;2:19–26.
41. Resnick SM, Sojkova J, Zhou Y, et al. Longitudinal cognitive decline is associated with fibrillar amyloid-beta measured by [11C]PiB. Neurology 2010;74:807–815.
42. Leal SL, Lockhart SN, Maass A, Bell RK, Jagust WJ. Subthreshold amyloid predicts tau deposition in aging. J Neurosci 2018;38:4482–4489.
43. Egan MF, Kost J, Voss T, et al. Randomized trial of verubecestat for prodromal Alzheimer's disease. N Engl J Med 2019;380:1408–1420.
44. Hanseeuw BJ, Betensky RA, Mormino EC, et al. PET staging of amyloidosis using striatum. Alzheimers Dement 2018;14:1281–1292.
45. Palmqvist S, Mattsson N, Hansson O. Cerebrospinal fluid analysis detects cerebral amyloid-β accumulation earlier than positron emission tomography. Brain 2016;139:1226–1236.
46. Racine AM, Koscik RL, Nicholas CR, et al. Cerebrospinal fluid ratios with Aβ 42 predict preclinical brain β-amyloid accumulation: Alzheimer's dement diagnosis. Alzheimers Dement (Amst) 2016;2:27–38.
47. Mattsson N, Insel PS, Donohue M, et al. Independent information from cerebrospinal fluid amyloid-β and florbetapir imaging in Alzheimer's disease. Brain 2015;138:772–783.
48. Palmqvist S, Zetterberg H, Blennow K, et al. Accuracy of brain amyloid detection in clinical practice using cerebrospinal fluid β-amyloid 42: a cross-validation study against amyloid positron emission tomography. JAMA Neurol 2014;71:1282–1289.
49. Toledo JB, Bjerke M, Da X, et al. Nonlinear association between cerebrospinal fluid and florbetapir F-18 β-amyloid measures across the spectrum of Alzheimer disease. JAMA Neurol 2015;72:571–581.

This information is current as of March 18, 2020

Updated Information & Services	including high resolution figures, can be found at: http://n.neurology.org/content/94/14/e1512.full
References	This article cites 49 articles, 10 of which you can access for free at: http://n.neurology.org/content/94/14/e1512.full#ref-list-1
Citations	This article has been cited by 1 HighWire-hosted articles: http://n.neurology.org/content/94/14/e1512.full##otherarticles
Subspecialty Collections	This article, along with others on similar topics, appears in the following collection(s): **Alzheimer's disease** http://n.neurology.org/cgi/collection/alzheimers_disease **Class II** http://n.neurology.org/cgi/collection/class_ii
Permissions & Licensing	Information about reproducing this article in parts (figures,tables) or in its entirety can be found online at: http://www.neurology.org/about/about_the_journal#permissions
Reprints	Information about ordering reprints can be found online: http://n.neurology.org/subscribers/advertise

AMERICAN ACADEMY OF NEUROLOGY®